SvedbergOpen
DISSEMINATION OF KNOWLEDGE
International Journal of Artificial Intelligence and Machine Learning
Publisher's Home Page: https://www.svedbergopen.com/

Research Paper Open Access

Innovative Biodegradable PVA–Starch Films Reinforced With Clay And Lime: Advancing Sustainable Packaging For Climate Resilience

Noshabah Tabassum[1,*], Maria Qayyum[1], Iqra Safdar[1], Tanzeela Tahir[1]

[*1] Fatima Jinnah Women University, Department of Environmental Sciences, The Mall, Rawalpindi, Pakistan.
*Corresponding Authors: noshabatabassum@fjwu.edu.pk

Abstract: Heightened global apprehension over the environmental pollution of conventional plastics and its undesirable effects on climate has accelerated research interest in biodegradable polymeric materials. In this study, bioplastic films derived from starch and polyvinyl alcohol (PVA) were reinforced with varying concentrations of calcium oxide (CaO) commonly known as lime and bentonite clay aiming to improve structural and functional properties. Bioplastic films were systemically evaluated with respect to mechanical strength, thermal behavior, moisture retention, water absorption and biodegradable behavior. Among all the formations the sample containing elevated amount of both CaO and bentonite (S7) exhibited the most favorable properties profile, attaining the tensile strength of 18.7 MPa and elongation at break of 93.19%, with thermal degradation commenced above 300 °C, reflecting noticeable thermal resistance. In contrast the high bentonite–low CaO (S47) sample demonstrated the lowest water absorption (21.8%) and moisture retention (8.21%), indicating strong barrier performance. In soil burial tests, S7 film demonstrated maximum degradation after 60 days, indicating great biodegradability. Scanning Electron Microscopy (SEM) revealed clear morphological variation among the selected samples, FTIR analysis confirmed the interaction of fillers and the PVA-starch films, while Principal Component Analysis (PCA) effectively distinguished performance relationships among formulations. K-means clustering further classified S7 with in high performance group. This integrated analytical approach underscores the prospective capabilities of dual-filler reinforcement in enhancing properties of biofilms. The results provide valuable insights into designing sustainable packaging materials as alternatives to petroleum-based plastics.

Keywords: Bioplastics, Sustainable Materials, Green Polymers, Principal Component Analysis, biodegradation.

1. Introduction

By the year 2025, global plastic waste is expected to reach 460 million tons annually due to rising consumption and insufficient recycling efforts. Each year, over 380 million tons of plastic are produced, of which approximately 91% is not recycled. According to recent estimates, between 75 million and 199 million tons of plastic waste actively contributes to the pollution of the world's oceans, with an increment of 15 million tons (approximately 33 billion pounds) entering the marine ecosystem every year (Fleck, 2024). If this pattern persists, annual plastic pollution is expected to exceed 1.1 billion tons by 2050, causing serious threats to the environment (Geyer et al., 2017; Market Data: Plastics Europe, 2018).

To minimize the environmental impacts induced by traditional plastics, their attention is growing in bioplastics manufactured from renewable biomass that can decompose in natural environment and have lower carbon footprint (Ibrahim et al., 2021). Among these, starch-based bioplastics have received notable attraction due to the easy accessibility of starch, its low cost, and its biodegradability (Muthusamy & Pramasivam, 2019). However, pure starch-based bioplastic exhibits limited water resistance, mechanical strength, and heat resistance, which constrain their practical applications (Zoumaki et al., 2019). To reduce limitations, starch is often blended with biodegradable polymers such as polyvinyl alcohol (PVA), a semi crystalline, hydrophilic polymer known for its notable film forming efficiency, outstanding gas barrier efficiency, and high tensile strength exceeding 70 MPa (Kausar, 2020). The abundant hydroxyl groups (-OH) present in PVA facilitates hydrogen bonding with starch molecules, increase intermolecular interaction, and overall structural stability. PVA has also been integrated with many additives such as glycerol, chitosan, polyethylene glycol (PEG), and fillers such as nano clays to enhance film properties for application needs (Teodorescu et al., 2018; Azizati & Haqiqi, 2021).

Bentonite and CaO are emerging as effective candidates as fillers. Bentonite, a layered aluminosilicate upon exfoliating or intercalating with in polymer blend, generates nanostructured composites that increase tensile strength (up to 50 MPa) and enhance barrier properties by limiting gas and water vapor permeability (Pech-Cohuo et al., 2024).

Similarly, calcium oxide (CaO) or lime, a strong and reactive alkaline compound, can form interaction with hydroxyl groups when incorporated with starch and PVA polymer matrix to promote crosslinking, thereby enhancing structural framework. Addition of CaO enhances thermal resistance (elevating degradation temperatures above 250 °C), while simultaneously reducing moisture content, and in some cases, imparts antimicrobial capabilities. Its incorporation developed the formation of compact polymer networks through ionic bridge, which not only significantly reduces water uptake but also increases the durability of the films (Achenef et al., 2024).

Although PVA, starch, bentonite, and calcium oxide (CaO) have each been studied individually in the development of biopolymers, no previous research has examined the combined effect of all these components within a single film matrix. The uniqueness of this study lies in its investigation of the synergistic use of both bentonite and CaO as dual reinforcing agents in PVA starch composite films.

To better understand the effect of compositional factors on the overall functionality of the bioplastic, this study employed multivariant analysis tool such as: Principal Component Analysis (PCA). PCA helps to identify the main elements that most strongly affect film characteristics such as tensile strength, moisture susceptibility, and biodegradability (Greenacre et al., 2022).

In this study, PCA not only highlighted the relationship among different film formulations and their measured properties but also facilitates in grouping or clustering same type of samples and revealing clear performance trends. This multivariate data analysis provided a deeper understanding of how the combined incorporation of bentonite clay and calcium oxide modulates the performance of the starch PVA bioplastic film.

2. Materials and Methods

2.1. Materials

Starch was extracted from potato peels using a slightly modified method based on Arikan and Bilgen (BEZİRHAN ARIKAN & BİLGEN, 2019). The extracted starch was then purified, dried, and stored in airtight containers for future use. Polyvinyl alcohol (PVA) (molecular weight 85,000–124,000; 99+% hydrolyzed; viscosity 28–32 cps), glycerol (molecular weight 92.09; purity ≥99.0%), calcium oxide (CaO) (≥99.9%, Reagent Plus, loss on ignition ≤10%), and bentonite clay (particle size ≤75 µm; pH 8.5–9.5) were procured from Sigma-Aldrich (Merck KGaA, Germany). All materials were used as received, without any further purification.

2.2. Preparation of a bioplastic film

Bioplastic films are made using the solvent casting technique. The first step of this process involved dissolving PVA in 100 mL of distilled water at 100 °C for 120 minutes under constant stirring at 600 rpm, using a JOAN LAN (OSC-10L) instrument. Once the PVA was completely dissolved, the pre-measured amounts of bentonite clay, calcium oxide, and starch were added to the solution along with glycerol (3% by weight), and the mixture was continuously stirred at 70 °C and 600 rpm until it became viscous.

The solution was then allowed to cool and cast onto petri plate. The cast film was then left at room temperature for 48 hours to allow the solvent to evaporate completely. Once dried, the film was carefully removed from the sheet. The experiment was conducted under atmospheric conditions with a temperature of 35 ± 2 °C and relative humidity of 28–31%. The main objective of this research was to evaluate the impact of bentonite clay and calcium oxide on the quality of the bioplastic film. Therefore, all physico-chemical properties of the films were tested to determine the optimal conditions for the film fabrication process "Table 1". To ensure the accuracy of experiment the selective picture of samples based on the low and high concentration of fillers were shown on which characterization methods were employed "Figure 1".

Table 1. Experimental design its parameters and responses.

Parameter					Response				
Sample	**Starch (g)**	**PVA (g)**	**CaO (g)**	**Bentonite (g)**	**MC (%)**	**WA (%)**	**TS (MPa)**	**Elongation (%)**	**Biodegradation (%)**
S1	2	4	1.25	0.53	19.84	30.43	10.7	53.28	65.27
S2	2	4	0.9	1.94	12.86	62.19	13	102.48	34.34

			9						72.47
S3	2	4	2.85	0.79	11.86	52.14	4.59	62.92	54.75
S4	2	4	2.93	0.88	17.37	49.53	4.96	64.52	80.01 67.3
S5	2	4	2.38	2.96	20.23	40.42	7.83	93.22	98.2
S6	2	4	2.31	2.31	15.19	38.69	12.92	48.91	75.49 72.98
S7	2	4	3.16	3.4	24.67	43.77	18.7	93.19	33.19
S8	2	4	2.78	2.58	19.64	55.66	11.3	111.03	81.5 63.72
S9	2	4	1.04	3.43	16.18	64.4	15.82	95.7	57.68
S10	2	4	0.95	2.05	14.67	47.97	8.77	75.23	81.23 56.75
S11	2	4	1.81	2.07	13.83	55.12	7.75	75.06	61.27
S12	2	4	1.66	0.85	20.39	51.37	8.31	101.21	41.81 50.89
S13	2	4	2.23	1.5	15.46	53.12	5.57	85.25	84.96
S14	2	4	0.94	1.32	9.01	55.36	15.44	46.79	42.15 57.12
S15	2	4	2.56	3.11	14.77	62.91	8.08	86.61	94.29
S16	2	4	1.91	0.76	20.55	28.74	11.29	105.19	45.38 89.59
S17	2	4	2.21	1.94	11.1	59.37	11.68	66.97	89.7
S18	2	4	2.44	3.01	10.98	35.96	10.82	114.21	35.93 60.14
S19	2	4	2.67	2.03	17.04	33.74	3.04	100.06	62.64
S20	2	4	2.54	0.65	17.04	50.76	17.83	85.93	50.39 33.08
S21	2	4	1.04	2.34	18.78	29.31	16.58	100.13	45.71

S22	2	4	0.85	1.72	22.44	64.84	6.11	46.33	36.21
									45.49
S23	2	4	1.23	2.64	20.32	53.23	7.39	108.75	
									82.51
S24	2	4	0.52	0.77	18.39	57.55	4.08	105.72	88.17
									32.81
S25	2	4	1.58	1.65	20.28	25.73	16.53	112.79	
									49.63
S26	2	4	0.94	0.57	13.49	51.75	17.75	50.29	93.74
									65.07
S27	2	4	2.13	1.66	14.15	50.06	6.86	46.54	
									70.71
S28	2	4	3.07	0.93	11.88	32.15	11.47	51.07	30.36
									61.52
S29	2	4	1.1	1.17	12.99	31.89	15.1	71.95	
									94.24
S30	2	4	0.9	2.88	18.73	56.3	8.92	73.94	
									54.39
S31	2	4	1.14	2.65	9.57	39.34	13.97	84.98	
									36.31
S32	2	4	3.42	1.95	15.37	56.14	5.42	49.78	60.02
									46.6
S33	2	4	3.07	3.44	15.32	49.95	12.01	56.11	
									52.22
S34	2	4	2.1	2.78	16.39	42.5	15.99	104.93	
S35	2	4	1.8	0.77	15.24	66.63	17.75	77.44	
S36	2	4	1.06	2.11	13.31	62.88	4.19	104.64	
S37	2	4	1.36	2.53	15.25	41.08	9.43	40.59	
S38	2	4	2.38	2.72	23.19	26.96	6.07	84.13	
S39	2	4	1.57	2.38	24.05	38.71	9.76	114.55	
S40	2	4	2.69	3.15	16.53	42.92	11.22	86.57	
S41	2	4	2.17	2.9	18.61	56.72	4.4	56.49	
S42	2	4	3.3	2.16	9.97	69.79	7.45	97.42	

			3						
S43	2	4	0.96	3.11	13.39	41.02	16.91	70.32	
S44	2	4	3.19	1.73	15.05	59.31	11.54	93.47	
S45	2	4	1.03	0.7	22.73	51.69	9.86	42.35	
S46	2	4	2.28	0.92	12.26	56.13	14.3	90.87	
S47	2	4	0.63	3.49	8.21	21.8	14.13	42.58	
S48	2	4	2.46	1.09	24.75	42.95	3.73	99.58	
S49	2	4	1.6	3.16	16.83	35.84	13.63	77.83	81.93
S50	2	4	2.89	3	18.42	40.46	15.59	49.74	81.93

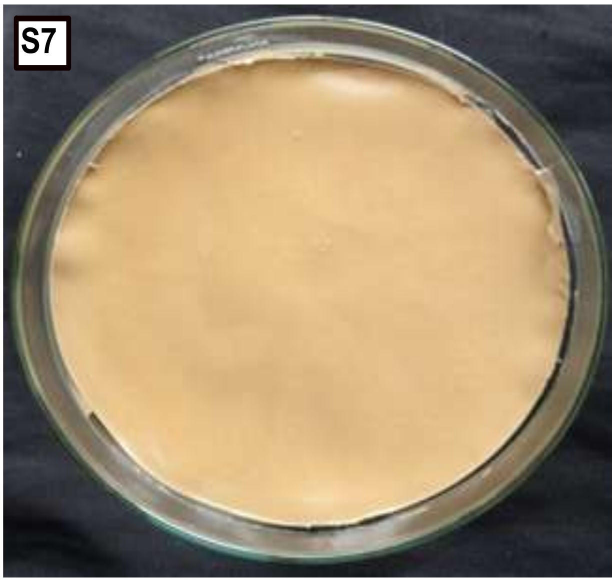

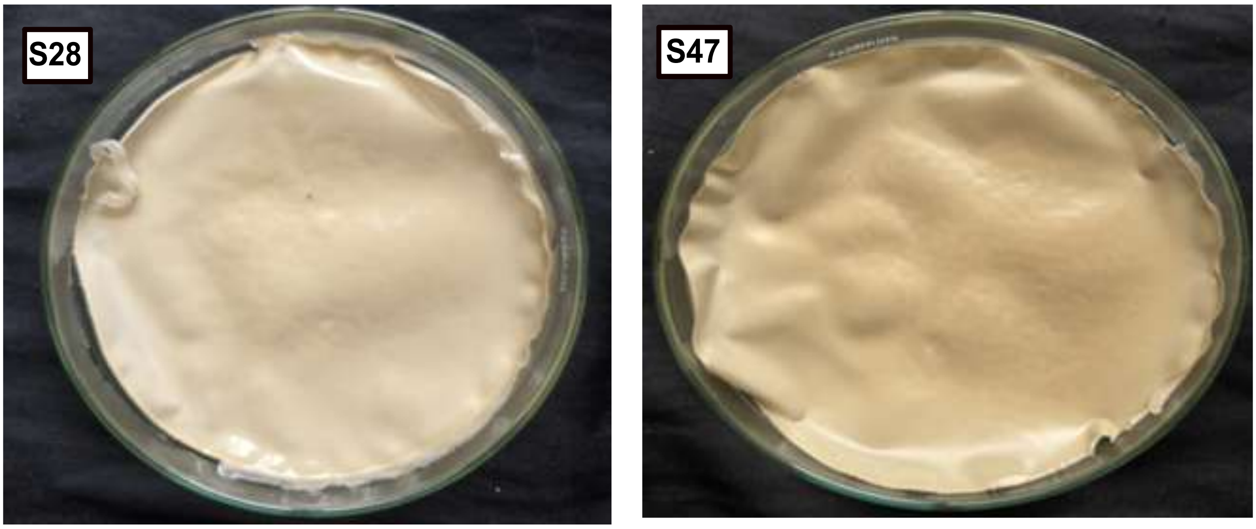

Figure 1. The bioplastic film samples with varying concentration of CaO and Bentonite clay

2.3. Multivariate Statistical Analysis: PCA and K-Means Clustering

Principal Component Analysis (PCA) was conducted using GraphPad Prism version 10.5.0(774), to standardize data by using correlation matrix and reduce data dimensionality. The first two principal components (PC1 and PC2) explained majority of variance and these distributions were visualized in 2-dimensional biplots with confidence ellipses, allowing clear clustering patterns based on different film formulations (Lin et al., 2015). K-means clustering was employed to further classify the 50 samples into distinct groups, with the optimal number of clusters determined using the elbow method (Liu et al., 2023). The identify groups were mapped on to the PCA plot properly visualized natural separations in response behavior among formulations.

3. Characterization techniques

3.1. Thermal Analysis

Thermal resistance of four different film samples was evaluated using a Simultaneous TGA–DSC analyzer (SDT Q600, TA Instruments, New Castle, DE, USA). Approximately sample weighing 10 - 30 mg was placed in a platinum pan and subjected to controlled heating from room temperature up to 700 °C at a rate of 10 °C per minute under a nitrogen atmosphere (Drelich et al., 2020).

3.2. Fourier Transform Infrared Spectroscopy (FTIR)

Fourier Transform Infrared (FTIR) spectroscopy was carried out using an FTIR spectrophotometer (SHIMADZU 8300, Kyoto, Japan). Spectra were recorded over the wavelength range of 4000 to 400 cm^{-1} at a resolution of 4 cm^{-1}. Every sample was examined in solid form to analyze characteristic absorption bands corresponding to chemical interactions between the polymer matrix and incorporated fillers (Prakash Bhuyar et al., 2019).

3.3. Scanning Electron Microscopy

The surface morphology and material formulation of bioplastic films were evaluated using a Scanning Electron Microscope (SEM) (MIRA3 TESCAN, Brno, Czech Republic). Each sample was fixed on aluminum stumbling using dual side tape and then sputter-coated with a thin layer of gold (10 to 20 nm) to enhance electrical conduction. SEM images were obtained at an accelerating voltage in the range of 5 - 10 kV, with a spatial resolution of approximately 5 nm.

4. Physical Chemical Analysis

4.1. Mechanical Analysis

The tensile strength (TS, MPa) and elongation at break (EAB, %) of bioplastic films were evaluated in accordance with the ASTM D882-12 protocol using a WAW-500E automatic hydraulic testing system machine. This testing instrument has a peak load capacity of 500 kN with deformation measurement with an efficiency of ±1% (Admase et al., 2022; Mittal et al., 2020). Flat clamps suitable for film thicknesses up to 30 mm were used during analysis. The film samples (S7, S24, S28, and S47) were cut into 100 mm strips and preconditioned at 24 °C and 50% moisture level for 72 hours prior to testing. The tensile test was starting with an initial grip of 40 mm, and the rate of displacement was constant at 0.2 kN/s (Gadhave et al., 2019). A photoelectric encoder was used to convert mechanical displacement into digital output, ensuring accurate measurement of the films' tensile properties.

4.2. Water Absorption Analysis

The water absorption behavior of films was assessed by using adapted process describe by Shen et al. (2010). The test was performed by soaking dry film samples (50 × 50 mm) in 100 mL of distilled water at room temperature for 24 hours. After immersion, the excess water was meticulously wiped using Whatman filter paper, and the wet weight (Ww) of each sample was measured. The dry weight (Wd) had been measured beforehand. The water absorption percentage (WA%) was calculated by using the following formula (Balavairavan et al., 2023):

$$WA\ (\%) = [(Ww - Wd) / Wd] \times 100 \quad (1)$$

4.3. Moisture Content

The moisture or water content (MC%) of the bioplastic samples was evaluated gravimetrically. Films (40 mm × 40 mm) were initially dried at 50 °C, and their dry mass (M_1) was obtained. The dried samples were then set in a desiccator containing a saturated sodium chloride (NaCl) solution, which maintained a constant relative humidity (RH) of 75%. After 24 hours, the films were weighed again to obtain the final mass (M_2) (Ge et al., 2020). The moisture content was determined by using the following formula:

$$MC\ (\%) = [(M_2 - M_1) / M_1] \times 100 \quad (2)$$

4.4. Soil Burial Degradability

Film samples size 4 × 4 cm^2 were subjected to a soil burial testing to determine their biodegradability. The samples were buried at a depth level of 10 cm in soil under controlled parameters, such as temperature of 30 °C, a pH of 6.5, and a relative humidity of 60%. The biodegradation process of the samples was monitored over a specific time to evaluate their decomposition behavior under natural environmental conditions (Al-Salem et al., 2019; Pech-Cohuo et al., 2024).

5. Result and discussion

5.1. Integrated PCA 2D bi plots Showing Grouping Behavior

In each 2D biplot, samples are projected onto PC1 and PC2, which together account for approximately 40.8% of the total variance (with PC1 explaining about 21.5% and PC2 around 19.3%). The arrows (loading vectors) represent the original variables, with their direction and length indicating the strength and influence of each variable on sample positioning; the angles between arrows reflect the correlations among variables (Bigi et al., 2021) “Figure 2”.

When grouped by tensile strength, samples with higher strength cluster along the positive side of PC2, opposite to elongation, indicating a trade-off between stiffness and ductility. Grouping based on moisture content and water absorption shows that samples with higher moisture cluster in the direction of the moisture and absorption loadings, opposite to the high-strength region. Grouping by bentonite clay reveals that samples with higher clay content align negatively along PC1 with biodegradation, confirming clay’s role in moisture interaction and degradation rate. Grouping by elongation shows that samples with lower elongation align with higher strength, while those with greater elongation group with increased biodegradability and clay content. Finally, grouping based on biodegradability shows that highly biodegradable samples cluster near the clay and elongation vectors but away from tensile strength and moisture resistance. Confidence ellipses surrounding each group illustrate their homogeneity and variability tight ellipses indicate uniform groups, while larger or overlapping ellipses reveal greater within-group variation and gradual transitions between property levels (Deng et al., 2022).

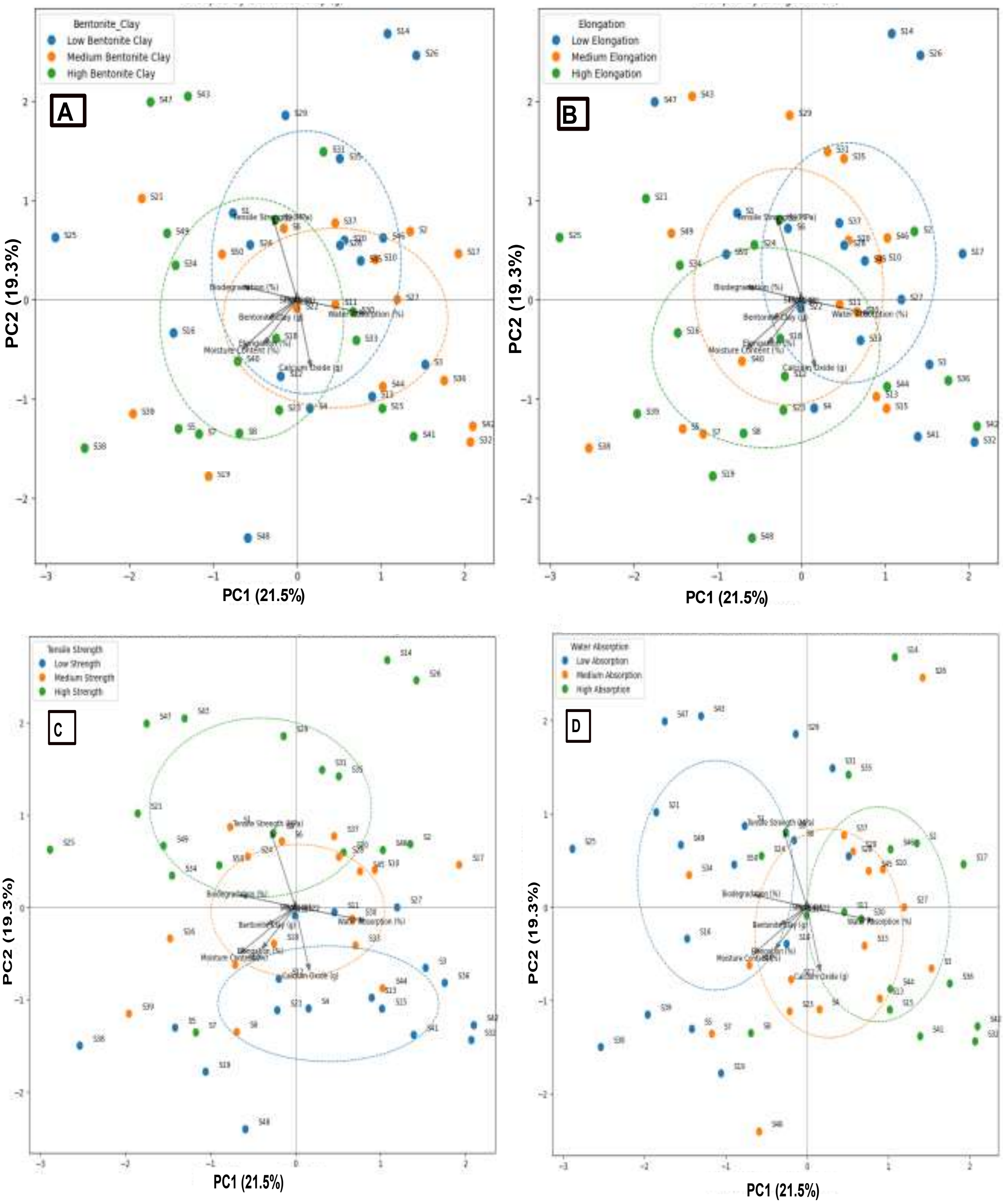
A
Bentonite_Clay
Low Bentonite Clay
Medium Bentonite Clay
High Bentonite Clay
B
Elongation
Low Elongation
Medium Elongation
High Elongation
C
Tensile Strength
Low Strength
Medium Strength
High Strength
D
Water Absorption
Low Absorption
Medium Absorption
High Absorption
Tensile Strength (MPa)
Biodegradation (%)
Bentonite Clay (g)
Water Absorption (%)
Moisture Content (%)
Calcium Oxide (g)
PC1 (21.5%)
PC2 (19.3%)

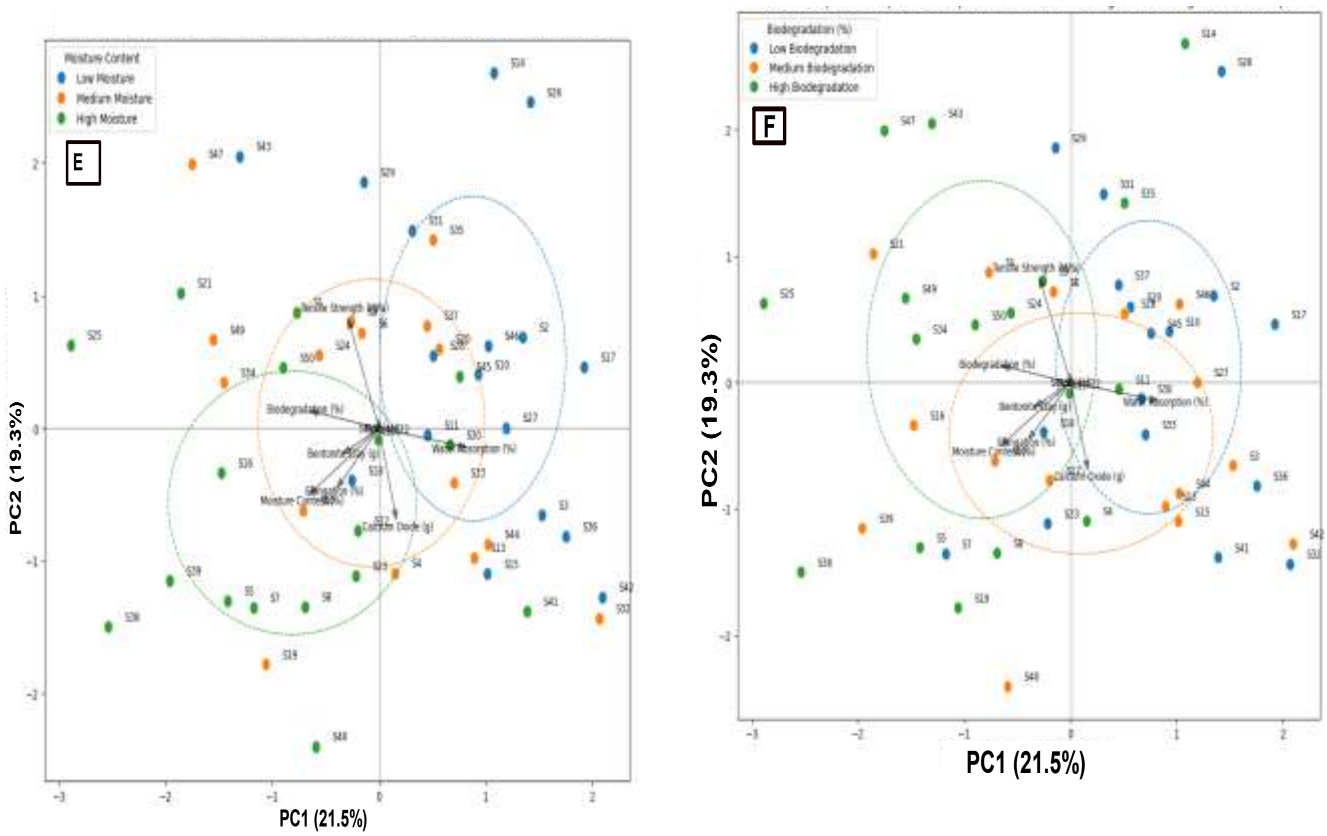

Figure 2. 2D biplot of PCA analysis (A) sample grouped by bentonite clay (B) sample grouped by elongation (C) sample grouped by tensile strength (D) sample grouped by water absorption (E) sample grouped by water content (F) sample grouped by biodegradation.

5.2. K-mean Clustering Using PCA

The Principal Component Analysis (PCA) biplots with K-means cluster coloring clearly illustrate how the three clusters (Cluster 0, Cluster 1, and Cluster 2) are distributed based on key variables "Figure 3". Cluster 0 (purple) occupies negative side of PC1 and PC2 and is linked with higher tensile strength and elevated bentonite clay content, reflecting robust and reinforced material properties. Cluster 1 (blue) is placed between the other clusters, representing samples with intermediate levels of strength, moisture, and biodegradability. Cluster 2 (yellow) placed positively along PC1 and PC3, indicating higher calcium oxide content and water absorption, which concede increased moisture uptake and biodegradability (Figure 4). The clustering graphs show that samples within each cluster are mostly grouped closely, demonstrating homogeneity, while slight dispersion of samples depict its natural variation (Rutolo et al., 2014). Although PCA suggested that calcium oxide notably contributes to total variation, its lack of significant differences across clusters indicates that its role is more synergistic, enhancing the effect of bentonite clay rather than acting independently (Du et al., 2023; Lim et al., 2024).

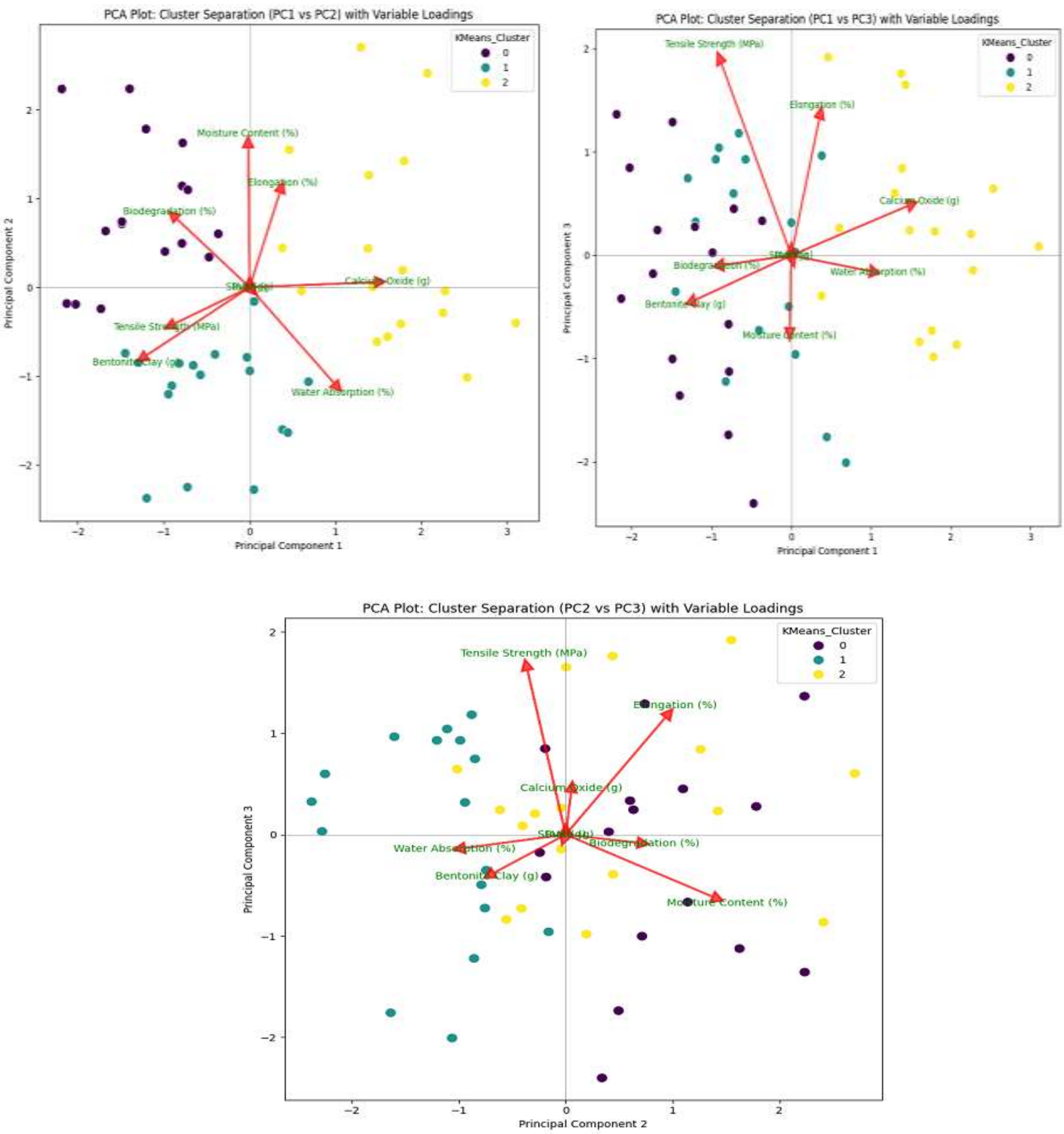

Figure 3. K means clustering between PCA1, PCA2, and PCA3

5.3. Fourier Transform Infrared (FTIR) Spectroscopy Analysis

All spectra exhibited characteristic peaks attributed to the polymer matrix (starch and PVA), along with variations caused by different levels of CaO and bentonite (S7, S24, S28, and S47), confirming the successful integration of both fillers into the polymer network "Figure 4".

A wide absorption band located at 3500 cm^{-1}, attributed to O–H stretching vibrations modes because of hydroxyl groups present in starch, PVA, water, and surface hydroxyls of clay and CaO, was deducted in all bioplastic samples. This band was Significantly wide and strong in bioplastic film with high bentonite and low CaO (S47) content, due to the water loving nature and high surface area of bentonite, which enhance extensive hydrogen bonding. Conversely, samples rich in CaO and low in bentonite (S28) shows a less border O–H band, along with a sharp peak at 3640 cm^{-1}, characteristic of $Ca(OH)_2$ formed by limited hydration of CaO (Trache et al., 2020). This peak was most pronounced in CaO-rich films, indicating interaction with atmospheric water and suggesting enhancing ionic mobility within the

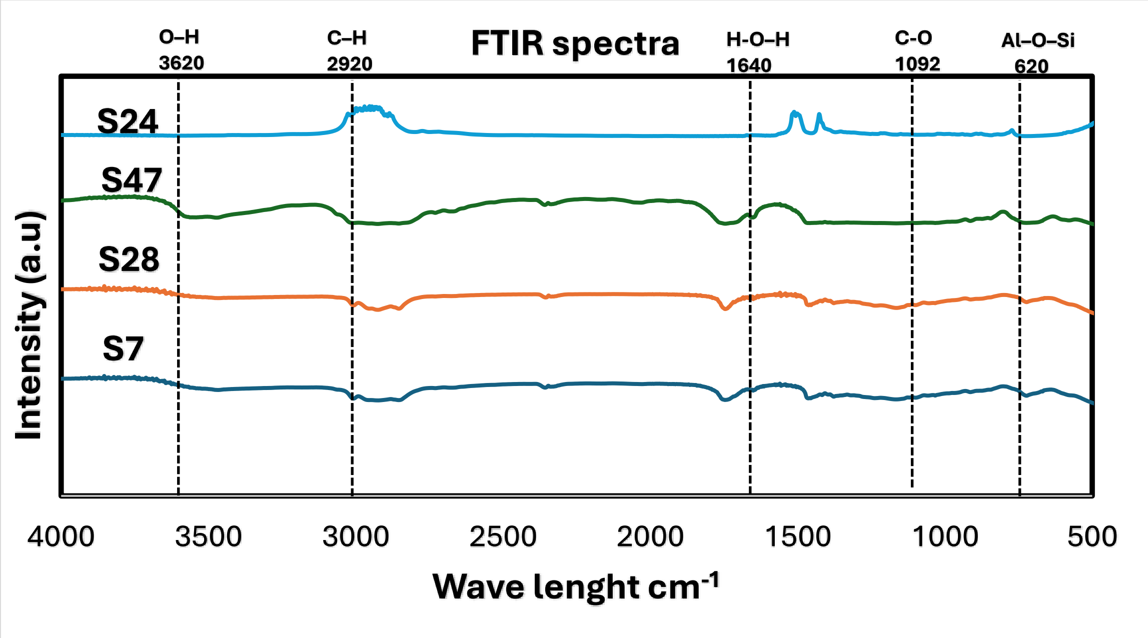

Figure 4. FTIR spectra of samples S7, S24, S28, and S47.

polymer network. C–H stretching vibrations near 2900 cm^{-1}, associated with the aliphatic chains in PVA and starch, were consistently present across all samples and showed negligible changes with varying filler composition. A band at 1640 cm^{-1}, corresponding to the bending of adsorbed water molecules (H–O–H), appeared in all spectra, confirming the hydrophilic character of both the polymer matrix and the incorporated fillers. Within the fingerprint region, all samples exhibited prominent C–O stretching bands at 1095 cm^{-1} indicative of the polymer backbone (Lu et al., 2019). Bending vibrations such as Al–O–Si, observed in the 400–600 cm^{-1} range, further confirmed the presence of clay. The film containing both high CaO and bentonite content (S7) displayed overlapping features from both fillers, including a pronounced $Ca(OH)_2$ peak at ~3640 cm^{-1} and enhanced Si–O and Al–O–Si signals, producing a complex spectrum with broadened peaks, particularly in the O–H and fingerprint regions (Zhao et al., 2018). This suggests synergistic interactions between the inorganic components and the polymer matrix, potentially improving structural cohesion and composite performance. Conversely, the low CaO and bentonite sample (S24) showed significantly weaker inorganic-related peaks, with spectra dominated by sharper polymer bands, especially in the 1000–1200 cm^{-1} range, indicating minimal filler incorporation. This simpler composition may be advantageous for applications requiring flexibility, optical clarity, and ease of processing.

5.4. Scanning Electron Microscopy (SEM) analysis

Surface morphology of the bioplastic films containing different ratios of calcium oxide (CaO) and bentonite clay was examined using Scanning Electron Microscopy (SEM) (Abbas et al., 2021) "Figure 5".The sample with high CaO and low bentonite (S28) displayed a rough and irregular texture with prominent CaO clusters, indicating successful additive incorporation, which could improve thermal behavior and facilitate controlled degradation. In contrast, the high-bentonite, low-CaO sample (S47) exhibited a consistent, flake-like pattern, characteristic of well-dispersed bentonite, which likely enhances structural integrity and barrier properties (Ma et al., 2020). The sample containing elevated levels of both CaO and bentonite (S7) presented a complex, interconnected architecture, combining CaO aggregates with organized, stacked bentonite layers. This structure implies synergistic interactions between the two fillers, potentially improving tensile strength, adsorption efficiency, and thermal stability (Wijaya et al., 2021). Conversely, the low-CaO, low-bentonite sample (S24) had a smooth, uniform surface, reflecting minimal disruption to the polymer matrix. This simpler morphology supports increased flexibility and transparency, making it suitable for lightweight or optically clear applications (Yari et al., 2021; Rammak et al., 2021). Overall, SEM results demonstrate that both the type and proportion of fillers play a crucial role in shaping the surface features of bioplastic films. Strategic adjustment of additive composition enables tailoring of functional properties for targeted applications (Wu et al., 2022).

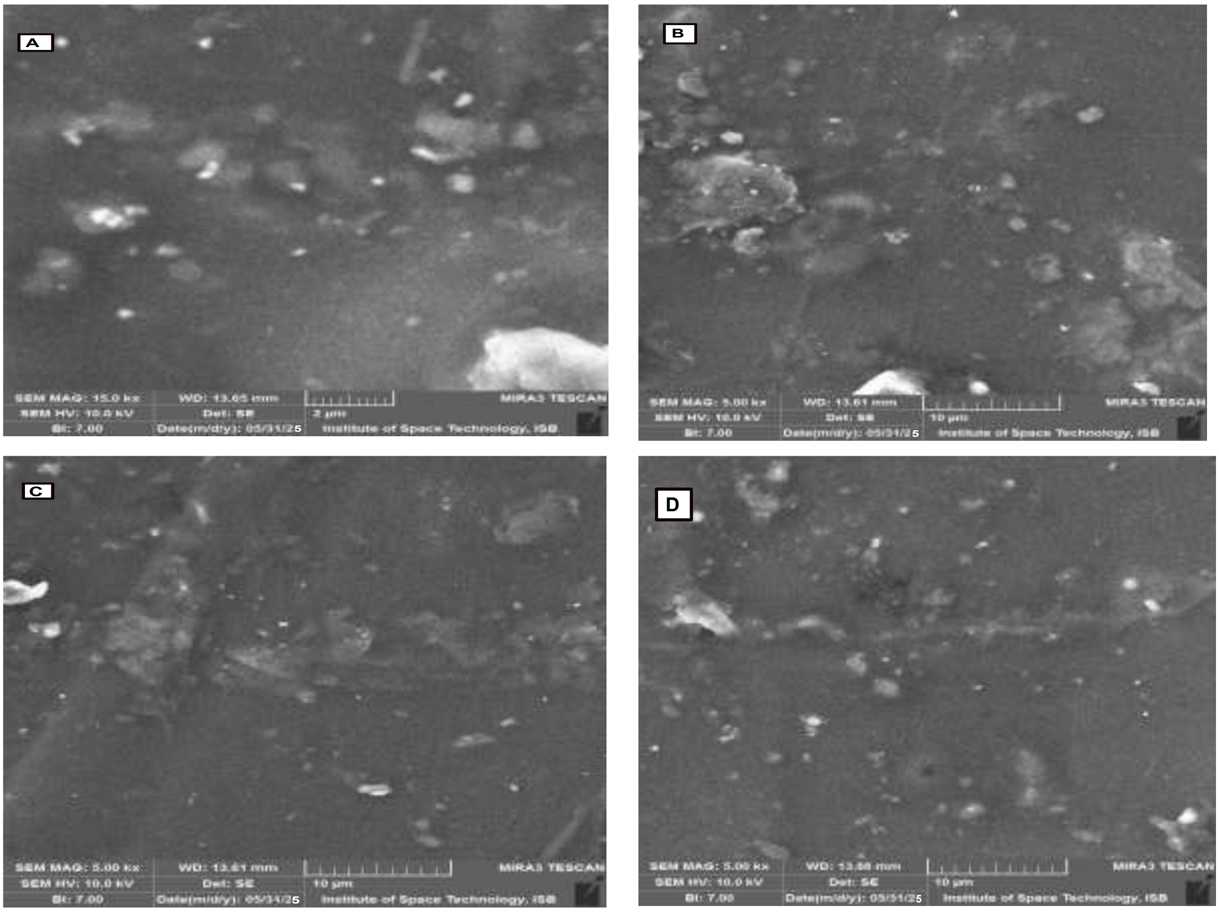

Figure 5. SEM analysis (A) S24 (low CaO and low Bentonite) (B) S47 (low CaO and high bentonite) (C) S7 (high CaO and high bentonite) (D) S28 (high CaO and low bentonite).

5.5. Thermal gravimetric analysis

The TGA thermograms of all bioplastic films displayed a distinct three-phase thermal degradation profile, corresponding to moisture loss, polymer decomposition, and breakdown of inorganic constituents "Figure 6". During the first stage (30–200 °C), weight loss primarily occurred due to evaporation of surface-bound water and loosely associated hydroxyl groups (Benabbou et al., 2024; António Benjamim Mapossa et al., 2023). Among the tested formulations, the sample S47(blue) showed the greatest initial mass loss at 13%, reflecting the high-water retention capacity of bentonite. The sample S28 (red) exhibited a similar but slightly lower loss (12%), likely caused by partial hydration of CaO to form $Ca(OH)_2$. The sample S7 (green) lost approximately 11%, while the sample S24 (orange) displayed the smallest initial weight change (6.5%), indicating minimal water affinity due to its low filler content.

The second degradation phase (200–400 °C) accounted for the largest weight reduction, associated with thermal decomposition of the starch and PVA polymer chains. The sample S24 (orange) underwent the highest polymer degradation (40%) due to the absence of significant thermal reinforcement. In contrast, the sample S7 (green) experienced only 28% mass loss, suggesting improved thermal stability from synergistic interactions between the two fillers (Yu et al., 2021). The S28 (red) and S47 (blue) samples showed intermediate losses of 32% and 30%, respectively, indicating moderate stabilization from individual additives.

During the final stage (400–600 °C), the decomposition shifted from organic material breakdown to structural transformations of the fillers. CaO-rich samples (red and green) showed an additional weight loss of 7–10%, corresponding to thermal decomposition of Ca $(OH)_2$ to CaO and water at around 450–500 °C. Bentonite-rich films (blue and green) also underwent further mass loss of 9–12%, attributed to dihydroxylation of the aluminosilicate layers. The S24 (orange) displayed minimal change (~6.5%), as most of its mass had decomposed earlier.

At 700 °C, the remaining mass reflected the residual inorganic content. The S7 (green) maintained the highest char (27.7%), confirming enhanced structural stability from dual-filler reinforcement. The 47 (blue) and 28 (red) films remained 24.5% and 21.4%, respectively, while the S24 (orange) left the lowest residue (16.8%), highlighting its limited thermal resistance and minimal inorganic content (Dai et al., 2017).

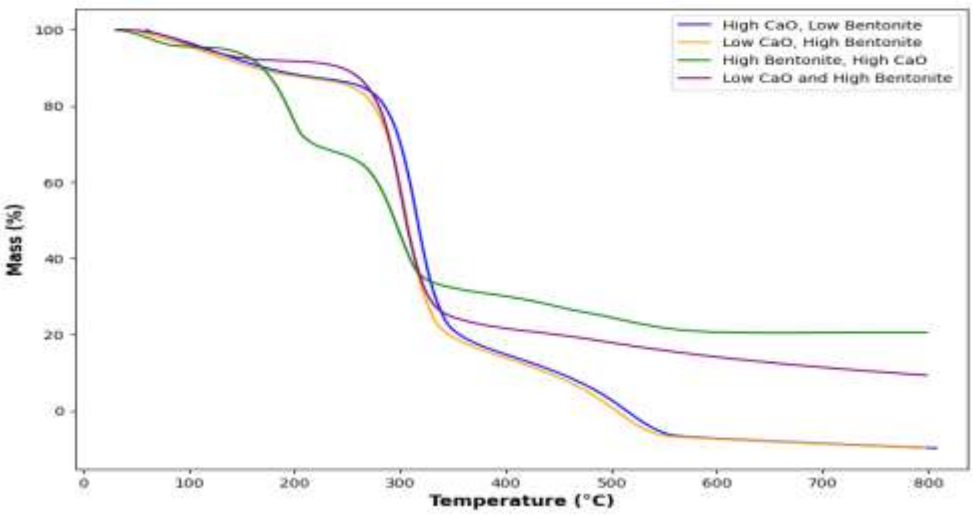

Figure 6. TGA analysis (A) high cao and low bentonite value in sample (B) low CaO and high bentonite value in sample (C) high CaO and high bentonite value in sample (D) low CaO and high bentonite value in sample.

6. Conclusion

In conclusion, the performance of starch–PVA-based bioplastic films is strongly governed by the concentration of calcium oxide (CaO) and bentonite clay. Films containing high levels of both fillers (S7) exhibited superior mechanical properties, achieving a tensile strength of 18.7 MPa and elongation at break of 93.19%, while the Low CaO–Low Bentonite (S24) films displayed the weakest mechanical performance. Thermal analysis confirmed that dual high-filler films possess enhanced heat resistance, with degradation onset above 300 °C and a gradual mass loss, reflecting improved thermal stability. Moisture and water resistance were similarly influenced by filler composition. High bentonite content imparted excellent barrier properties, with the High Bentonite–Low CaO (S47) film showing the low water absorption (21.8%) and moisture content (8.21%), whereas high CaO–low bentonite (28) formulations absorbed more water, highlighting bentonite's role in improving compactness and hydrophilicity. Biodegradability tests indicated that the High CaO–High Bentonite films (S7) degraded most efficiently, losing 98.2% of their mass within 60 days while retaining initial structural integrity. Conversely, films with low CaO and high bentonite (S47) degraded more slowly due to denser matrices and limited porosity. Multivariate analysis using PCA and K-means clustering confirmed these trends, consistently identifying the high dual-filler films as a distinct high-performance group and the low dual-filler films as the lowest-performing cluster.Overall, combining CaO and bentonite in optimal proportions allows for the development of starch–PVA bioplastics with balanced mechanical strength, thermal stability, water resistance, and biodegradability, offering a promising approach for sustainable material design.

Acknowledgments:

The author sincerely acknowledges the Higher Education Commission (HEC) of Pakistan for providing financial support for this research under the Technology Development Fund project (TDF-478).

References

1. Abbas, M. I., Sountharapandiyan, N. G., & Khudus, S. T. (2021). Surface Bacterial Adhesion Study of Novel Ternary PVC/ Polyester/ Bentonite Clay Nanocomposite Films. Current Physical Chemistry, 11(1), 35–44. https://doi.org/10.2174/1877946810999200616125951
2. Admase, A. T., Sendekie, Z. B., & Alene, A. N. (2022). Biodegradable Film from Mango Seed Kernel Starch Using Pottery Clay as Filler. Journal of Polymers and the Environment, Volume 30, pages 3431–3446, (2022). https://doi.org/10.1007/s10924-022-02449-7
3. Al-Salem, S. M., Sultan, H. H., Karam, H. J., & Al-Dhafeeri, A. T. (2019). Determination of biodegradation rate of commercial oxo-biodegradable polyethylene film products using ASTM D 5988. Journal of Polymer Research, 26(7), N.PAG–N.PAG.
https://doi.org/10.1007/s10965-019-1822-5
4. António Benjamim Mapossa, Júnior, S., Rafael, C., & Washington Mhike. (2023). Thermal, Morphological and Mechanical Properties of Multifunctional Composites Based on Biodegradable Polymers/Bentonite Clay: A Review. Polymers, 15(16), 3443–3443.
https://doi.org/10.3390/polym15163443
5. Azizati, Z., & Haqiqi, A. K. (2021). Synthesis and characterization of bioplastic based on chitosan-urea-bentonite. Journal of Physics: Conference Series, 1796(1), 012108.

https://doi.org/10.1088/1742-6596/1796/1/012108
6. Balavairavan, B., Saravanakumar, S. S., Senthamaraikannan, P., Indran, S., & Siengchin, S. (2023). Evaluation of physiochemical, mechanical, thermal, UV barrier, and biodegradation properties of PVA/corn (Zea mays) cob powder biofilms. Biomass Conversion and Biorefinery, 14(19), 24611–24622. https://doi.org/10.1007/s13399-023-04404-5
7. Benabbou, A., Bourassi, L., Yahyaoui, M. I., Merimi, I., Challioui, A., Asehraou, A., & Siaj, M. (2024). Enhancement of bioplastic properties using metal-ligand coordination for applications in food packaging. Interactions, 245(1). https://doi.org/10.1007/s10751-024-02140-4
8. BEZİRHAN ARIKAN, E., & BİLGEN, H. D. (2019). Production of bioplastics from potato peel waste and investigation of its biodegradability. International Advanced Research and Engineering Journal, 3(2), 93–97. https://doi.org/10.35860/iarej.420633
9. Bigi, F., Haghighi, H., De Leo, R., Ulrici, A., & Pulvirenti, A. (2021). Multivariate exploration data analysis by PCA of the combined effect of film-forming composition, drying conditions, and UV-C irradiation on the functional properties of films based on chitosan and pectin. LWT, 137(February 2021), 110432. https://doi.org/10.1016/j.lwt.2020.110432
10. Dai, L., He, C., Wang, Y., Liu, Y., Yu, Z., Zhou, Y., Fan, L., Wang, H., & Ruan, R. (2017). Comparative study on microwave and conventional hydrothermal pretreatment of bamboo sawdust: Hydrochar properties and its pyrolysis behaviors. Energy Conversion and Management, 146(146 (1–7) (2017)), 1–7. https://doi.org/10.1016/j.enconman.2017.05.007
11. Deng, H., He, R., Huang, R., Pang, C., Ma, Y., Xia, H., Liang, D., Liao, L., Xiong, B., Wang, X., Zhang, M., Ao, X., Yu, B., Han, D., & Wang, Z. (2022). Optimization of a static headspace GC-MS method and its application in metabolic fingerprinting of the leaf volatiles of 42 citrus cultivars. Frontiers in Plant Science, 13(December 202213:1050289). https://doi.org/10.3389/fpls.2022.1050289
12. Drelich, J., Malgorzata Urszula Sikora-Jasinska, Ehsan Mostaed, Liu, H., Maier, P., Seitz, J., & Hort, N. (2020). Biodegradable Materials for Medical Applications II. JOM, 72(5), 1830–1832. https://doi.org/10.1007/s11837-020-04129-0
13. Du, B.-X., Long, Y., Li, X., Wu, M., & Shi, J.-Y. (2023). CMMS-GCL: cross-modality metabolic stability prediction with graph contrastive learning. Bioinformatics, 39(8). https://doi.org/10.1093/bioinformatics/btad503
14. Felicia Omolara Afolabi, Musonge, P., & Babatunde Femi Bakare. (2021). Bio-sorption of a bi-solute system of copper and lead ions onto banana peels: characterization and optimization. Journal of Environmental Health Science and Engineering, 19(1), 613–624. https://doi.org/10.1007/s40201-021-00632-x
15. Fleck, A. (2024, June 7). Infographic: The World Is Flooded With Plastic Waste. Statista Daily Data. https://www.statista.com/chart/32385/global-plastic-waste-production-by-application/
16. Gadhave, R. V., Mahanwar, P. A., & Gadekar, P. T. (2019). Effect of glutaraldehyde on thermal and mechanical properties of starch and polyvinyl alcohol blends. Designed Monomers and Polymers, 22(1), 164–170. https://doi.org/10.1080/15685551.2019.1678222
17. Ge, X., Chang, M., Jiang, W., Zhang, B., Xing, R., & Bulin, C. (2020). Selective location of kaolin and effects of maleic anhydride in kaolin/poly(ε-caprolactone)/poly(lactic acid) composites. Applied Clay Science, 189(Volume 189, May 2020, 105524), 105524–105524. https://doi.org/10.1016/j.clay.2020.105524
18. Geyer, R., Jambeck, J. R., & Law, K. L. (2017). Production, use, and fate of all plastics ever made. Science Advances, 3(7). https://doi.org/10.1126/sciadv.1700782
19. Greenacre, M., Groenen, P. J. F., Hastie, T., D'Enza, A. I., Markos, A., & Tuzhilina, E. (2022). Principal component analysis. Nature Reviews Methods Primers, 2(1), 1–21. https://doi.org/10.1038/s43586-022-00184-w
20. Habtamu Asmare Achenef, Shimelis Admassu Emire, Kassahun, S. K., & Kim, H. (2024). Enset starch-based biocomposite film reinforced with Ethiopian bentonite clay: Improved mechanical and barrier properties. International Journal of Biological Macromolecules, Volume 287(January 2025, 138499), 138499–138499. https://doi.org/10.1016/j.ijbiomac.2024.138499
21. Ibrahim, N. I., Shahar, F. S., Sultan, M. T. H., Shah, A. U. M., Safri, S. N. A., & Mat Yazik, M. H. (2021). Overview of Bioplastic Introduction and Its Applications in Product Packaging. Coatings, 11(11), 1423. https://doi.org/10.3390/coatings11111423
22. Kausar, A. (2020). Innovations in Poly(Vinyl Alcohol) Derived Nanomaterials. Advances in Materials Science, 20(3), 5–22. https://doi.org/10.2478/adms-2020-0013
23. Lim, A. M. W., Lim, E. U., Chen, P.-L., & Fann, C. S. J. (2024). Unsupervised clustering identified clinically relevant

metabolic syndrome endotypes in UK and Taiwan Biobanks. IScience, 27(7), 109815. https://doi.org/10.1016/j.isci.2024.109815

24. Lin, Z., Wang, L., & Cao, J. (2015). Interpretable functional principal component analysis. Biometrics, 72(3), 846–854. https://doi.org/10.1111/biom.12457
25. Liu, H., Chen, J., Dy, J., & Fu, Y. (2023). Transforming Complex Problems into K-means Solutions. IEEE Transactions on Pattern Analysis and Machine Intelligence, Volume: 45(Issue: 7, 01 July 2023), 1–20. https://doi.org/10.1109/tpami.2023.3237667
26. Lu, J., Yang, Y., Liu, P., Li, Y., Huang, F., Zeng, L., Liang, Y., Li, S., & Hou, B. (2019). Iron-montmorillonite treated corn straw biochar: Interfacial chemical behavior and stability. The Science of the Total Environment, 708(, 708 (2020), 134773–134773. https://doi.org/10.1016/j.scitotenv.2019.134773
27. Luchese, C. L., Garrido, T., Spada, J. C., Tessaro, I. C., & de la Caba, K. (2018). Development and characterization of cassava starch films incorporated with blueberry pomace. International Journal of Biological Macromolecules, 106(January 2018,), 834–839. https://doi.org/10.1016/j.ijbiomac.2017.08.083
28. Ma, G., He, X., Jiang, X., Liu, H., Chu, J., & Xiao, Y. (2020). Strength and Permeability of Bentonite-Assisted Biocemented Coarse Sand. Canadian Geotechnical Journal, olume 58 • Number 7 • July 2021(July 2021). https://doi.org/10.1139/cgj-2020-0045
29. Market data:: PlasticsEurope. (2018). Plasticseurope.org. https://www.plasticseurope.org/en/resources/market-data
30. Mittal, A., Garg, S., & Bajpai, S. (2020). Fabrication and characteristics of poly (vinyl alcohol)-starch-cellulosic material based biodegradable composite film for packaging applications. Materials Today: Proceedings, 21(Volume 21, Part 3, 2020, Pages 1577-1582), 1577–1582. https://doi.org/10.1016/j.matpr.2019.11.210
31. None Haryanto, & Adinda Mariam Namira. (2025). Development of bioplastics from Durian seeds with the addition of carboxymethyl cellulose and bentonite. AIP Conference Proceedings, 3309(Issue 1), 020002–020002. https://doi.org/10.1063/5.0258501
32. Pech-Cohuo, S. C., Adrián, M., Pérez-Pacheco, E., André, J., Yasser Alejandro Chim-Chi, Ríos-Soberanis, C. R., Zujey Berenice Cuevas-Carballo, Erbin Guillermo Uc-Cayetano, Can-Herrera, L. A., Ortíz-Fernández, A., Collí-Pacheco, J. P., José Herminsul Mina-Hernández, & Yamile Pérez-Padilla. (2024). Effect of clays incorporation on properties of thermoplastic starch/clay composite bio-based polymer blends. Scientific Reports, 14(1). https://doi.org/10.1038/s41598-024-69092-1
33. Prakash Bhuyar, Nurul Aqilah Binti Mohd Tamizi, Mohd Hasbi Ab. Rahim, Gaanty Pragas Maniam, & Natanamurugaraj Govindan. (2019). Effect of ultraviolet light on the degradation of Low-Density and High-Density Polyethylene characterized by the weight loss and FTIR. Maejo International Journal of Energy and Environmental Communication, 1(2), 26–31. https://doi.org/10.54279/mijeec.v1i2.244915
34. Rammak, T., Boonsuk, P., & Kaewtatip, K. (2021). Mechanical and barrier properties of starch blend films enhanced with kaolin for application in food packaging. International Journal of Biological Macromolecules, 192(1 December 2021), 1013–1020. https://doi.org/10.1016/j.ijbiomac.2021.10.081
35. Rutolo, M. F., Covington, J. A., Clarkson, J. P., & Iliescu, D. (2014). Detection of Potato Storage Disease via Gas Analysis: A Pilot Study Using Field Asymmetric Ion Mobility Spectrometry. Sensors, 14(9), 15939–15952. https://doi.org/10.3390/s140915939
36. Selvamurugan Muthusamy, M., & Pramasivam, S. (2019). Bioplastics – An Eco-friendly Alternative to Petrochemical Plastics. Current World Environment, 14(1), 49–59. https://doi.org/10.12944/cwe.14.1.07
37. Shah, U., Gani, A., Ashwar, B. A., Shah, A., Ahmad, M., Gani, A., Wani, I. A., & Masoodi, F. A. (2015). A review of the recent advances in starch as active and nanocomposite packaging films. Cogent Food & Agriculture, 1(1), 1115640. https://doi.org/10.1080/23311932.2015.1115640
38. Shen, X. L., Wu, J. M., Chen, Y., & Zhao, G. (2010). Antimicrobial and physical properties of sweet potato starch films are incorporated with potassium sorbate or chitosan. Food Hydrocolloids, 24(4), 285–290. https://doi.org/10.1016/j.foodhyd.2009.10.003
39. Teodorescu, M., Bercea, M., & Morariu, S. (2018). Biomaterials of Poly(vinyl alcohol) and Natural Polymers. Polymer Reviews, 58(2), 247–287. https://doi.org/10.1080/15583724.2017.1403928
40. Trache, D., Tarchoun, A. F., Derradji, M., Hamidon, T. S., Masruchin, N., Brosse, N., & Hussin, M. H. (2020). Nanocellulose: From Fundamentals to Advanced Applications. Frontiers in Chemistry, 8(392). https://doi.org/10.3389/fchem.2020.00392
41. Wijaya, K., Maisari Utami, Akhmad Syoufian, & Murifal, A. I. (2021). Solid State Mixing Preparation of CaO/Bentonite Nanocomposite and its Application to Improve the Quality of Patchouli Oil. Advanced Materials Research, 1162(April 2021), 21–26. https://doi.org/10.4028/www.scientific.net/amr.1162.21

42. WU, Z., AMEER, K., HU, C., BAO, A., WANG, R., TANG, W., CHAUDHARY, N., & JIANG, G. (2022). Particle size of yam flour and its effects on physicochemical properties and bioactive compounds. Food Science and Technology, 42((2021), pp. 1-9).
https://doi.org/10.1590/fst.43921
43. Yari, S., Mohammadi-Rovshandeh, J., & Shahrousvand, M. (2021). Preparation and Optimization of Starch/Poly Vinyl Alcohol/ZnO Nanocomposite Films Applicable for Food Packaging. Journal of Polymers and the Environment, 30(4), 1502–1517.
https://doi.org/10.1007/s10924-021-02292-2
44. Yu, J., Wu, Z., An, X., Tian, F., & Yu, B. (2021). Trace metal elements mediated co-pyrolysis of biomass and bentonite for the synthesis of biochar with high stability. Science of the Total Environment, 774(20 June 2021), 145611.
https://doi.org/10.1016/j.scitotenv.2021.145611
45. Zhao, B., Xu, H., Zhang, T., Nan, X., & Ma, F. (2018). Effect of pyrolysis temperature on sulfur content, extractable fraction and release of sulfate in corn straw biochar. RSC Advances, 8(62), 35611–35617.
https://doi.org/10.1039/c8ra06382f
46. Zoumaki, M., Tzetzis, D., & Mansour, G. (2019). Development and characterization of starch - based nanocomposite materials. IOP Conference Series: Materials Science and Engineering, 564(1), 012037.
https://doi.org/10.1088/1757-899x/564/1/012037